

# UC Davis

## UC Davis Previously Published Works

### Title

Rotation-minimizing osculating frames

### Permalink

<https://escholarship.org/uc/item/3gx6x8nd>

### Journal

Computer Aided Geometric Design, 31(1)

### ISSN

0167-8396

### Authors

Farouki, Rida T  
Giannelli, Carlotta  
Sampoli, Maria Lucia  
[et al.](#)

### Publication Date

2014

### DOI

10.1016/j.cagd.2013.11.003

Peer reviewed

# Rotation–minimizing osculating frames

Rida T. Farouki

Department of Mechanical and Aerospace Engineering,  
University of California, Davis, CA 95616, USA.

Carlotta Giannelli

Institut für Angewandte Geometrie,  
Johannes Kepler Universität Linz,  
Altenberger Strasse 69, A–4040 Linz, AUSTRIA.

Maria Lucia Sampoli

Dipartimento di Ingegneria dell’Informazione e Scienze Matematiche,  
Università di Siena, Pian dei Mantellini 44, 53100 Siena, ITALY.

Alessandra Sestini

Dipartimento di Matematica e Informatica,  
Università degli Studi di Firenze,  
Viale Morgagni 67a, 50134 Firenze, ITALY.

## Abstract

An orthonormal frame  $(\mathbf{f}_1, \mathbf{f}_2, \mathbf{f}_3)$  is *rotation–minimizing* with respect to  $\mathbf{f}_i$  if its angular velocity  $\boldsymbol{\omega}$  satisfies  $\boldsymbol{\omega} \cdot \mathbf{f}_i \equiv 0$  — or, equivalently, the derivatives of  $\mathbf{f}_j$  and  $\mathbf{f}_k$  are both parallel to  $\mathbf{f}_i$ . The Frenet frame  $(\mathbf{t}, \mathbf{p}, \mathbf{b})$  along a space curve is rotation–minimizing with respect to the principal normal  $\mathbf{p}$ , and in recent years *adapted* frames that are rotation–minimizing with respect to the tangent  $\mathbf{t}$  have attracted much interest. This study is concerned with rotation–minimizing *osculating* frames  $(\mathbf{f}, \mathbf{g}, \mathbf{b})$  incorporating the binormal  $\mathbf{b}$ , and osculating–plane vectors  $\mathbf{f}, \mathbf{g}$  that have no rotation about  $\mathbf{b}$ . These frame vectors may be defined through a rotation of  $\mathbf{t}, \mathbf{p}$  by an angle equal to minus the integral of curvature with respect to arc length. In aeronautical terms,

the rotation–minimizing osculating frame (RMOF) specifies *yaw-free* rigid–body motion along a curved path. For polynomial space curves possessing rational Frenet frames, the existence of *rational* RMOFs is investigated, and it is found that they must be of degree 7 at least. The RMOF is also employed to construct a novel type of ruled surface, with the property that its tangent planes coincide with the osculating planes of a given space curve, and its rulings exhibit the least possible rate of rotation consistent with this constraint.

**Keywords:** rotation–minimizing frames; Pythagorean–hodograph curves; quaternions; angular velocity; rigid body motion; ruled surfaces.

e–mail: farouki@ucdavis.edu, carlotta.giannelli@jku.at,  
marialucia.sampoli@unisi.it, alessandra.sestini@unifi.it

# 1 Introduction

A general spatial motion of a rigid body is specified by describing its position and orientation as functions of time. A particular point of the body (e.g., the center of mass) is usually chosen to describe position. To describe orientation, the variation of an orthonormal frame ( $\mathbf{e}_1, \mathbf{e}_2, \mathbf{e}_3$ ) embedded within the body may be specified. In general, position and orientation vary independently, but in certain motion problems they may be correlated. This study is concerned with *constrained spatial motions*, in which the instantaneous angular velocity of a rigid body is related to the geometry of its center-of-mass path.

The *Frenet frame* is the most familiar orthonormal frame on a space curve, comprising the *tangent*  $\mathbf{t}$ , *principal normal*  $\mathbf{p}$ , and *binormal*  $\mathbf{b} = \mathbf{t} \times \mathbf{p}$ . When the Frenet frame is used to orient a body along a path, its angular velocity  $\boldsymbol{\omega}$  satisfies  $\boldsymbol{\omega} \cdot \mathbf{p} \equiv 0$  — i.e., it has no component in the principal normal direction. This means that the body exhibits no instantaneous rotation about the principal normal vector  $\mathbf{p}$  from point to point along the path.

In aerodynamics, an embedded frame is used [8] to characterize variations in the attitude of an aircraft, in terms of *roll*, *pitch*, and *yaw* axes through its center of mass — the roll (or longitudinal) axis is aligned with the fuselage; the pitch (or lateral) axis is orthogonal to it, within the plane of the fuselage and wings; and the yaw (or vertical) axis is orthogonal to that plane. Hence, pitch and yaw correspond to up/down and left/right motions of the aircraft nose, while roll corresponds to a rotation about the fuselage.

A rigid body that maintains alignment with the Frenet frame on a given spatial path exhibits a *pitch-free* motion — it has no instantaneous rotation about the principal normal  $\mathbf{p}$ . For a given (smooth) path, it is also possible to construct *roll-free* and *yaw-free* rigid-body motions, characterized by no instantaneous rotation about the tangent  $\mathbf{t}$  and binormal  $\mathbf{b}$ , respectively.

Roll-free motion, with angular velocity satisfying  $\boldsymbol{\omega} \cdot \mathbf{t} \equiv 0$ , has recently enjoyed considerable attention. In this case, the body has no instantaneous rotation about the tangent  $\mathbf{t}$  from point to point along the path. Bishop [5] first studied *adapted* orthonormal frames  $(\mathbf{t}, \mathbf{u}, \mathbf{v})$  comprising the tangent  $\mathbf{t}$  and normal-plane vectors  $\mathbf{u}, \mathbf{v}$  that have no instantaneous rotation about  $\mathbf{t}$ , in lieu of  $\mathbf{p}, \mathbf{b}$ . Klok [24] described the vectors  $\mathbf{u}, \mathbf{v}$  as solutions to differential equations, and Guggenheimer [20] subsequently showed that these solutions amount to defining  $\mathbf{u}, \mathbf{v}$  by a normal-plane rotation of  $\mathbf{p}, \mathbf{b}$  through an angle equal to minus the integral of the torsion with respect to arc length.

For polynomial or rational curves, this *rotation-minimizing adapted frame*

(RMAF) is not, in general, a rational locus, and this fact has prompted many approximation schemes [14, 23, 33]. More recently, interest has emerged in identifying curves with *rational* rotation–minimizing frames (RRMF curves), which must be *Pythagorean–hodograph* (PH) curves [9], since only PH curves possess rational unit tangents. The *Euler–Rodrigues frame* (ERF), a rational adapted frame defined on any PH curve, is a useful intermediary in identifying RRMF curves [6, 21]. The simplest non–planar RRMF curves form a subset of the PH quintics [11], characterized by the satisfaction of simple constraints on the curve coefficients [10]. Further details on the basic theory, properties, and applications of RRMF curves can be found in [1, 12, 17, 18].

Among the spatial motions mentioned above, in which angular velocity is correlated with local path geometry, the least–studied is the case of yaw–free motion satisfying  $\boldsymbol{\omega} \cdot \mathbf{b} \equiv 0$ . In yaw–free motion, the orientation of the body is specified by a frame  $(\mathbf{f}, \mathbf{g}, \mathbf{b})$  that retains the binormal  $\mathbf{b}$ , but the tangent and principal normal  $\mathbf{t}, \mathbf{p}$  are replaced by osculating–plane vectors  $\mathbf{f}, \mathbf{g}$  that have no instantaneous rotation about  $\mathbf{b}$ . It is shown below that the vectors  $\mathbf{f}, \mathbf{g}$  can be defined through an osculating–plane rotation of  $\mathbf{t}, \mathbf{p}$  by an angle equal to minus the integral of the curvature with respect to arc length. We call the frame  $(\mathbf{f}, \mathbf{g}, \mathbf{b})$  a *rotation–minimizing osculating frame* (RMOF).

The plan for the remainder of this paper is as follows. Section 2 describes the concept of rotation–minimizing frames on curves, and briefly mentions how it can also be used to identify certain special curves on a smooth surface (geodesics, lines of curvature, and asymptotic lines). Section 3 addresses the problem of *rational* rotation–minimizing frames — after briefly reviewing rational RMAFs, a detailed analysis of rational RMOFs on cubic and quintic space curves with rational Frenet frames is presented. Section 4 employs the RMOF to construct ruled surfaces interpolating a space curve, with tangent planes matching the osculating planes of that curve, and derives some useful properties of such surfaces. Finally, Section 5 summarizes the key results of this study, and identifies some open problems.

## 2 Rotation–minimizing frames on curves

The *parametric speed* of a differentiable space curve  $\mathbf{r}(\xi)$  is defined by

$$\sigma(\xi) = |\mathbf{r}'(\xi)| = ds/d\xi,$$

where  $s$  is the cumulative arc length of  $\mathbf{r}(\xi)$ , measured from some fixed point. The curve  $\mathbf{r}(\xi)$  is *regular* if its parametric speed satisfies  $\sigma(\xi) \neq 0$  for all  $\xi$ . The variation of an orthonormal frame  $(\mathbf{e}_1(\xi), \mathbf{e}_2(\xi), \mathbf{e}_3(\xi))$  defined along  $\mathbf{r}(\xi)$  may be specified by its angular velocity  $\boldsymbol{\omega}(\xi)$  through the relations

$$\mathbf{e}'_1 = \sigma \boldsymbol{\omega} \times \mathbf{e}_1, \quad \mathbf{e}'_2 = \sigma \boldsymbol{\omega} \times \mathbf{e}_2, \quad \mathbf{e}'_3 = \sigma \boldsymbol{\omega} \times \mathbf{e}_3. \quad (1)$$

Since  $(\mathbf{e}_1, \mathbf{e}_2, \mathbf{e}_3)$  comprise a basis for  $\mathbb{R}^3$  we can write

$$\boldsymbol{\omega} = \omega_1 \mathbf{e}_1 + \omega_2 \mathbf{e}_2 + \omega_3 \mathbf{e}_3, \quad (2)$$

and hence the relations (1) become

$$\mathbf{e}'_1 = \sigma(\omega_3 \mathbf{e}_2 - \omega_2 \mathbf{e}_3), \quad \mathbf{e}'_2 = \sigma(\omega_1 \mathbf{e}_3 - \omega_3 \mathbf{e}_1), \quad \mathbf{e}'_3 = \sigma(\omega_2 \mathbf{e}_1 - \omega_1 \mathbf{e}_2). \quad (3)$$

For a given *reference direction*, specified by a unit vector field  $\mathbf{c}(\xi)$  along  $\mathbf{r}(\xi)$ , one may characterize frames  $(\mathbf{e}_1(\xi), \mathbf{e}_2(\xi), \mathbf{e}_3(\xi))$  that are *rotation-minimizing* with respect to  $\mathbf{c}(\xi)$  as follows.

**Definition 1.** The frame  $(\mathbf{e}_1, \mathbf{e}_2, \mathbf{e}_3)$  is *rotation-minimizing* with respect to  $\mathbf{c}$  if its angular velocity  $\boldsymbol{\omega}$  has no component in the direction of  $\mathbf{c}$ , i.e.,  $\boldsymbol{\omega} \cdot \mathbf{c} \equiv 0$ .

Now if the frame vector  $\mathbf{e}_1(\xi)$  is chosen as the reference direction, the rotation-minimizing frame (RMF) satisfies  $\omega_1 \equiv 0$  in (2). Equations (3) then yield an alternative characterization, in terms of the derivatives of  $\mathbf{e}_2(\xi)$  and  $\mathbf{e}_3(\xi)$ .

**Corollary 1.** The frame  $(\mathbf{e}_1, \mathbf{e}_2, \mathbf{e}_3)$  is *rotation-minimizing* with respect to  $\mathbf{e}_1$  when  $\mathbf{e}'_2$  or  $\mathbf{e}'_3$  is always parallel to  $\mathbf{e}_1$  along the curve  $\mathbf{r}(\xi)$ . An analogous characterization holds when  $\mathbf{e}_2$  or  $\mathbf{e}_3$  is chosen as the reference direction.

For a frame that is rotation-minimizing with respect to  $\mathbf{e}_1$ , the vectors  $\mathbf{e}_2, \mathbf{e}_3$  exhibit no instantaneous rotation about  $\mathbf{e}_1$ . They vary only because  $\mathbf{e}_1$  varies along  $\mathbf{r}(\xi)$ , and they must remain orthogonal to it. This is equivalent to the observation in Corollary 1 that the derivatives of  $\mathbf{e}_2, \mathbf{e}_3$  are parallel to  $\mathbf{e}_1$ .

The *Frenet frame*  $(\mathbf{t}, \mathbf{p}, \mathbf{b})$  on a space curve  $\mathbf{r}(\xi)$  is defined [25] by

$$\mathbf{t} = \frac{\mathbf{r}'}{|\mathbf{r}'|}, \quad \mathbf{p} = \frac{\mathbf{r}' \times \mathbf{r}''}{|\mathbf{r}' \times \mathbf{r}''|} \times \mathbf{t}, \quad \mathbf{b} = \frac{\mathbf{r}' \times \mathbf{r}''}{|\mathbf{r}' \times \mathbf{r}''|}. \quad (4)$$

The *tangent*  $\mathbf{t}$  is the instantaneous direction of motion along the curve, the *principal normal*  $\mathbf{p}$  points to the *center of curvature*, and the *binormal*  $\mathbf{b} =$

$\mathbf{t} \times \mathbf{p}$  completes the frame. The orthogonal planes spanned by  $(\mathbf{t}, \mathbf{p})$ ,  $(\mathbf{p}, \mathbf{b})$ , and  $(\mathbf{b}, \mathbf{t})$  are the *osculating*, *normal*, and *rectifying* planes, respectively.

The angular velocity of the frame (4) is given [25] by the *Darboux vector*

$$\boldsymbol{\omega} = \kappa \mathbf{b} + \tau \mathbf{t}, \quad (5)$$

where the curvature  $\kappa(\xi)$  and torsion  $\tau(\xi)$  of  $\mathbf{r}(\xi)$  are defined by

$$\kappa = \frac{\mathbf{p} \cdot \mathbf{t}'}{\sigma} = \frac{|\mathbf{r}' \times \mathbf{r}''|}{|\mathbf{r}'|^3} \quad \text{and} \quad \tau = -\frac{\mathbf{p} \cdot \mathbf{b}'}{\sigma} = \frac{(\mathbf{r}' \times \mathbf{r}'') \cdot \mathbf{r}'''}{|\mathbf{r}' \times \mathbf{r}''|^2}.$$

When  $(\mathbf{e}_1, \mathbf{e}_2, \mathbf{e}_3) = (\mathbf{t}, \mathbf{p}, \mathbf{b})$  and  $\boldsymbol{\omega}$  is specified by (5), the relations (1) are equivalent [25] to the well-known *Frenet–Serret equations*

$$\begin{bmatrix} \mathbf{t}' \\ \mathbf{p}' \\ \mathbf{b}' \end{bmatrix} = \sigma \begin{bmatrix} 0 & \kappa & 0 \\ -\kappa & 0 & \tau \\ 0 & -\tau & 0 \end{bmatrix} \begin{bmatrix} \mathbf{t} \\ \mathbf{p} \\ \mathbf{b} \end{bmatrix}. \quad (6)$$

**Remark 1.** From Definition 1, we observe that the Frenet frame is rotation–minimizing with respect to the principal normal  $\mathbf{p}$ , but not with respect to the tangent  $\mathbf{t}$  or binormal  $\mathbf{b}$ . For a plane curve, it is also rotation–minimizing with respect to the tangent  $\mathbf{t}$ .

Although the Frenet frame is not rotation–minimizing with respect to  $\mathbf{t}$ , one can easily derive such a rotation–minimizing frame from it. New normal–plane vectors  $(\mathbf{u}, \mathbf{v})$  are specified through a rotation of  $(\mathbf{p}, \mathbf{b})$  according to

$$\mathbf{u} = \cos \theta \mathbf{p} + \sin \theta \mathbf{b}, \quad \mathbf{v} = -\sin \theta \mathbf{p} + \cos \theta \mathbf{b}, \quad (7)$$

where [20] we define

$$\theta(\xi) = \theta_0 - \int_0^\xi \tau \sigma \, d\xi, \quad (8)$$

$\theta_0$  being an integration constant — note that the minus sign is missing from (8) in [20]. It is assumed in (7) that  $\mathbf{r}(\xi)$  is free of inflections, so  $\mathbf{p}$  and  $\mathbf{b}$  are defined at each point. The frame  $(\mathbf{t}, \mathbf{u}, \mathbf{v})$  has angular velocity

$$\boldsymbol{\omega} = \kappa \mathbf{b} = \kappa (\sin \theta \mathbf{u} + \cos \theta \mathbf{v}), \quad (9)$$

satisfying  $\boldsymbol{\omega} \cdot \mathbf{t} \equiv 0$ . A frame incorporating the tangent  $\mathbf{t}$  is an *adapted* frame, and when it is rotation–minimizing with respect to  $\mathbf{t}$  it is called a *rotation–minimizing adapted frame* (RMAF). Such frames describe natural spatial

motions of a rigid body that maintains one principal axis aligned with the path tangent, while the other principal axes have no instantaneous rotation about the tangent. These motions are useful in computer animation, the use of sweep operations in geometric design, robot path planning, programming of CNC machines with rotary axes, and related applications.

By modification of the Frenet frame, one can also define a frame that is rotation-minimizing with respect to the binormal  $\mathbf{b}$ . New osculating-plane vectors  $(\mathbf{f}, \mathbf{g})$  are specified through a rotation of  $(\mathbf{t}, \mathbf{p})$  according to

$$\mathbf{f} = \cos \theta \mathbf{t} + \sin \theta \mathbf{p}, \quad \mathbf{g} = -\sin \theta \mathbf{t} + \cos \theta \mathbf{p}, \quad (10)$$

where, in this case, we define

$$\theta(\xi) = \theta_0 - \int_0^\xi \kappa \sigma \, d\xi. \quad (11)$$

Using  $\theta' = -\sigma\kappa$  and (6), the variation of  $(\mathbf{f}, \mathbf{g}, \mathbf{b})$  is described by  $\mathbf{f}' = \sigma \boldsymbol{\omega} \times \mathbf{f}$ ,  $\mathbf{g}' = \sigma \boldsymbol{\omega} \times \mathbf{g}$ ,  $\mathbf{b}' = \sigma \boldsymbol{\omega} \times \mathbf{b}$ , where the frame angular velocity is

$$\boldsymbol{\omega} = \tau \mathbf{t} = \tau (\cos \theta \mathbf{f} - \sin \theta \mathbf{g}). \quad (12)$$

Evidently  $\boldsymbol{\omega} \cdot \mathbf{b} \equiv 0$ , and this frame is rotation-minimizing with respect to  $\mathbf{b}$ . Since the vectors  $\mathbf{f}, \mathbf{g}$  span the osculating plane, and exhibit no instantaneous rotation about the normal  $\mathbf{b}$  to that plane along the curve  $\mathbf{r}(\xi)$ , we say that  $(\mathbf{f}, \mathbf{g}, \mathbf{b})$  is a *rotation-minimizing osculating frame* (RMOF).

**Example 1.** For the circular helix defined by

$$\mathbf{r}(\phi) = (R \cos \phi, R \sin \phi, k\phi) \quad (13)$$

the Frenet frame can be specified in terms of the parameters  $a = R/\sqrt{R^2 + k^2}$  and  $b = k/\sqrt{R^2 + k^2}$  as

$$\mathbf{t} = (-a \sin \phi, a \cos \phi, b), \quad \mathbf{p} = (-\cos \phi, -\sin \phi, 0), \quad \mathbf{b} = (b \sin \phi, -b \cos \phi, a)$$

and the parametric speed, curvature, and torsion are  $\sigma = \sqrt{R^2 + k^2}$ ,  $\kappa = a/\sigma$ ,  $\tau = b/\sigma$ . The angular deviation (8) of the RMAF normal-plane vectors  $(\mathbf{u}, \mathbf{v})$  from the Frenet frame vectors  $(\mathbf{p}, \mathbf{b})$  is thus  $\theta = \theta_0 - b\phi$ . Hence, for  $\theta_0 = 0$ , the RMAF basis vectors (7) are

$$\begin{aligned} \mathbf{u} &= (-\cos \phi \cos b\phi - b \sin \phi \sin b\phi, -\sin \phi \cos b\phi + b \cos \phi \sin b\phi, -a \sin b\phi), \\ \mathbf{v} &= (-\cos \phi \sin b\phi + b \sin \phi \cos b\phi, -\sin \phi \sin b\phi - b \cos \phi \cos b\phi, a \cos b\phi). \end{aligned}$$



Figure 1 compares the Frenet frame and RMAF normal-plane vectors along the helix (13) with  $R = 2.5$  and  $k = 0.6$ . The angular deviation (11) of the RMOF osculating-plane vectors ( $\mathbf{f}, \mathbf{g}$ ) from the Frenet frame vectors ( $\mathbf{t}, \mathbf{p}$ ) is  $\theta = \theta_0 - a\phi$ , and hence for  $\theta_0 = 0$  the RMOF basis vectors (10) are

$$\begin{aligned}\mathbf{f} &= (-a \sin \phi \cos a\phi + \cos \phi \sin a\phi, a \cos \phi \cos a\phi + \sin \phi \sin a\phi, b \cos a\phi), \\ \mathbf{g} &= (-a \sin \phi \sin a\phi - \cos \phi \cos a\phi, a \cos \phi \sin a\phi - \sin \phi \cos a\phi, b \sin a\phi).\end{aligned}$$

Figure 2 compares the Frenet frame and RMOF osculating-plane vectors.

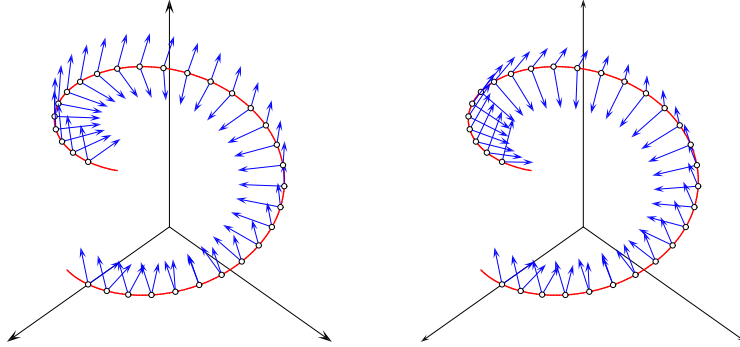


Figure 1: Comparison of (left) the Frenet frame vectors  $\mathbf{p}, \mathbf{b}$  and (right) the rotation-minimizing adapted frame vectors  $\mathbf{u}, \mathbf{v}$  on the circular helix (13).

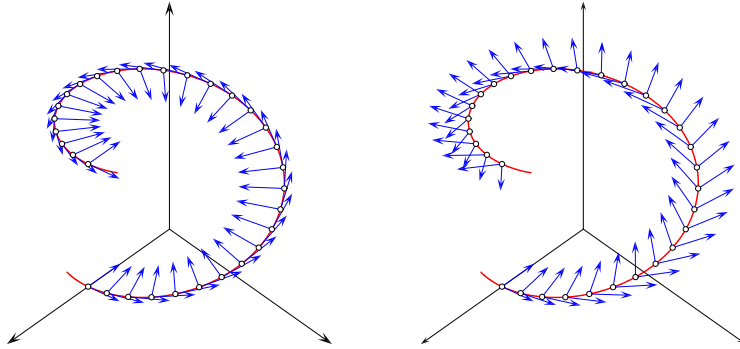


Figure 2: Comparison of (left) the Frenet frame vectors  $\mathbf{t}, \mathbf{p}$  and (right) the rotation-minimizing osculating frame vectors  $\mathbf{f}, \mathbf{g}$  on the circular helix (13).

For the Frenet frame ( $\mathbf{t}, \mathbf{p}, \mathbf{b}$ ) we have  $(\omega_1, \omega_2, \omega_3) = (\tau, 0, \kappa)$  from (5), so a body aligned with this frame along the path  $\mathbf{r}(\xi)$  exhibits *pitch-free* motion.

For the rotation–minimizing adapted frame  $(\mathbf{t}, \mathbf{u}, \mathbf{v})$  we have  $(\omega_1, \omega_2, \omega_3) = (0, \kappa \sin \theta, \kappa \cos \theta)$  from (9), so a body aligned with the RMAF exhibits *roll–free* motion. Finally, for the rotation–minimizing osculating frame  $(\mathbf{f}, \mathbf{g}, \mathbf{b})$  we have angular velocity components  $(\omega_1, \omega_2, \omega_3) = (\tau \cos \theta, -\tau \sin \theta, 0)$  from (12), and hence a body aligned with the RMOF exhibits *yaw–free* motion.

Rotation–minimizing frames can also offer intuitive characterizations for certain special curves on smooth surfaces. The *Darboux frame*  $(\mathbf{n}, \mathbf{t}, \mathbf{h})$  along a surface curve comprises the surface normal  $\mathbf{n}$ , the curve tangent  $\mathbf{t}$ , and the tangent normal  $\mathbf{h} = \mathbf{n} \times \mathbf{t}$  — i.e., a unit vector in the surface tangent plane, orthogonal to the curve tangent. The variation of the Darboux frame is specified [25, 32] in terms of its angular velocity

$$\boldsymbol{\Omega} = \kappa_g \mathbf{n} - \tau_g \mathbf{t} - \kappa_n \mathbf{h}$$

by the relations  $\mathbf{n}' = \sigma \boldsymbol{\Omega} \times \mathbf{n}$ ,  $\mathbf{t}' = \sigma \boldsymbol{\Omega} \times \mathbf{t}$ ,  $\mathbf{h}' = \sigma \boldsymbol{\Omega} \times \mathbf{h}$ , where

$$\kappa_g = \frac{\mathbf{h} \cdot \mathbf{t}'}{\sigma}, \quad \tau_g = \frac{\mathbf{h} \cdot \mathbf{n}'}{\sigma}, \quad \kappa_n = \frac{\mathbf{n} \cdot \mathbf{t}'}{\sigma},$$

are the *geodesic curvature*, *geodesic torsion*, and *normal curvature* along the surface curve. In terms of these quantities, the *geodesics*, *line of curvatures*, and *asymptotic lines* on a smooth surface may be characterized [25, 32] as loci along which  $\kappa_g \equiv 0$ ,  $\tau_g \equiv 0$ , and  $\kappa_n \equiv 0$ , respectively. From Definition 1, we obtain the following alternative succinct characterizations, which are useful in the construction of surface patches bounded by geodesics [19, 29, 31]; lines of curvature [4, 26, 27]; and asymptotic lines [2].

**Proposition 1.** *A surface curve is (i) a geodesic; (ii) a line of curvature; or (iii) an asymptotic line, if and only if the Darboux frame  $(\mathbf{n}, \mathbf{t}, \mathbf{h})$  is rotation–minimizing with respect to (i) the surface normal  $\mathbf{n}$ ; (ii) the curve tangent  $\mathbf{t}$ ; or (iii) the tangent normal  $\mathbf{h}$ .*

### 3 Rational rotation–minimizing frames

Exact rational frames are preferable to approximations when possible, since they provide a precise and efficient means of orienting a rigid body along a given path. After briefly reviewing the theory of rational RMAFs below, we consider its adaptation to the problem of identifying rational RMOFs.

### 3.1 Rational RMAF on PH curves

The existence of rational RMAFs on polynomial space curves has recently been studied [10]. A polynomial space curve with a rational RMAF must be a *Pythagorean-hodograph* (PH) curve, since only the PH curves have rational unit tangents [9]. The distinctive property of a polynomial PH curve  $\mathbf{r}(\xi) = (x(\xi), y(\xi), z(\xi))$  is that its derivative components satisfy [9] the condition

$$|\mathbf{r}'(\xi)|^2 = x'^2(\xi) + y'^2(\xi) + z'^2(\xi) = \sigma^2(\xi) \quad (14)$$

for some polynomial  $\sigma(\xi)$ . A spatial PH curve may be generated [7] from a quaternion polynomial

$$\mathcal{A}(\xi) = u(\xi) + v(\xi)\mathbf{i} + p(\xi)\mathbf{j} + q(\xi)\mathbf{k} \quad (15)$$

and its conjugate  $\mathcal{A}^*(\xi) = u(\xi) - v(\xi)\mathbf{i} - p(\xi)\mathbf{j} - q(\xi)\mathbf{k}$  through the product

$$\begin{aligned} \mathbf{r}'(\xi) = \mathcal{A}(\xi)\mathbf{i}\mathcal{A}^*(\xi) &= [u^2(\xi) + v^2(\xi) - p^2(\xi) - q^2(\xi)]\mathbf{i} \\ &+ 2[u(\xi)q(\xi) + v(\xi)p(\xi)]\mathbf{j} + 2[v(\xi)q(\xi) - u(\xi)p(\xi)]\mathbf{k}. \end{aligned} \quad (16)$$

Alternatively, one may use complex polynomials

$$\boldsymbol{\alpha}(\xi) = u(\xi) + \mathbf{i}v(\xi), \quad \boldsymbol{\beta}(\xi) = q(\xi) + \mathbf{i}p(\xi), \quad (17)$$

in the Hopf map expression

$$\mathbf{r}'(\xi) = (|\boldsymbol{\alpha}(\xi)|^2 - |\boldsymbol{\beta}(\xi)|^2, 2\operatorname{Re}(\boldsymbol{\alpha}(\xi)\overline{\boldsymbol{\beta}(\xi)}), 2\operatorname{Im}(\boldsymbol{\alpha}(\xi)\overline{\boldsymbol{\beta}(\xi)})). \quad (18)$$

**Lemma 1.** *If the complex polynomials in (18) are of the form  $\boldsymbol{\alpha}(\xi) = f(\xi)$ ,  $\boldsymbol{\beta}(\xi) = e^{i\psi}g(\xi)$  for real  $f(\xi)$ ,  $g(\xi)$  the curve defined by integrating (18) is planar. Furthermore, if  $g(\xi) = kf(\xi)$  for real  $k$ , it is just a straight line.*

**Proof :** When  $\boldsymbol{\alpha}(\xi) = f(\xi)$  and  $\boldsymbol{\beta}(\xi) = e^{i\psi}g(\xi)$  for constant  $\psi$ , we have

$$x'(\xi) = f^2(\xi) - g^2(\xi), \quad y'(\xi) = 2f(\xi)g(\xi)\cos\psi, \quad z'(\xi) = -2f(\xi)g(\xi)\sin\psi.$$

Since  $\sin\psi y'(\xi) + \cos\psi z'(\xi) = 0$ , we have  $\sin\psi y''(\xi) + \cos\psi z''(\xi) = 0$  and  $\sin\psi y'''(\xi) + \cos\psi z'''(\xi) = 0$ . Hence, the last two columns of the determinant

$$(\mathbf{r}'(\xi) \times \mathbf{r}''(\xi)) \cdot \mathbf{r}'''(\xi) = \begin{vmatrix} x'(\xi) & y'(\xi) & z'(\xi) \\ x''(\xi) & y''(\xi) & z''(\xi) \\ x'''(\xi) & y'''(\xi) & z'''(\xi) \end{vmatrix}$$

are linearly dependent, so the torsion vanishes and the curve is planar. Also, note that expression (18) reduces to  $\mathbf{r}'(\xi) = f^2(\xi) (1-k^2, 2k \cos \psi, -2k \sin \psi)$  if  $g(\xi) = kf(\xi)$ , which defines a straight line. Lemma 1 also holds in the case  $\boldsymbol{\alpha}(\xi) = e^{i\psi} f(\xi)$ ,  $\boldsymbol{\beta}(\xi) = g(\xi)$ . ■

On the PH curve defined by (15) and (16), a rational orthonormal adapted frame — the *Euler–Rodrigues frame* (ERF) — is defined [6] by

$$\mathbf{e}_1(\xi) = \frac{\mathcal{A}(\xi) \mathbf{i} \mathcal{A}^*(\xi)}{|\mathcal{A}(\xi)|^2}, \quad \mathbf{e}_2(\xi) = \frac{\mathcal{A}(\xi) \mathbf{j} \mathcal{A}^*(\xi)}{|\mathcal{A}(\xi)|^2}, \quad \mathbf{e}_3(\xi) = \frac{\mathcal{A}(\xi) \mathbf{k} \mathcal{A}^*(\xi)}{|\mathcal{A}(\xi)|^2}.$$

Here  $\mathbf{e}_1$  is the curve tangent while  $\mathbf{e}_2, \mathbf{e}_3$  span the normal plane. The variation of the ERF is characterized by its angular velocity  $\boldsymbol{\omega}$  through (1), where

$$\sigma(\xi) = |\mathbf{r}'(\xi)| = u^2(\xi) + v^2(\xi) + p^2(\xi) + q^2(\xi)$$

is the parametric speed of the PH curve  $\mathbf{r}(\xi)$ . Han [21] showed that the PH curve defined by (15)–(16) possesses a rational RMAF if and only if relatively prime polynomials  $a(\xi), b(\xi)$  exist, such that  $u(\xi), v(\xi), p(\xi), q(\xi)$  satisfy

$$\frac{uv' - u'v - pq' + p'q}{u^2 + v^2 + p^2 + q^2} = \frac{ab' - a'b}{a^2 + b^2}. \quad (19)$$

This is equivalent to the existence of a rational normal–plane rotation that maps the ERF vectors  $\mathbf{e}_2(\xi), \mathbf{e}_3(\xi)$  onto the RMAF vectors  $\mathbf{u}(\xi), \mathbf{v}(\xi)$  so the ERF angular velocity component in the  $\mathbf{e}_1$  direction is exactly cancelled. For PH quintics, specified by quadratic quaternion polynomials with Bernstein coefficients  $\mathcal{A}_0, \mathcal{A}_1, \mathcal{A}_2$ , the condition for a rational RMAF may be expressed [10] as a single constraint on these coefficients, namely

$$\mathcal{A}_2 \mathbf{i} \mathcal{A}_0^* + \mathcal{A}_0 \mathbf{i} \mathcal{A}_2^* = 2 \mathcal{A}_1 \mathbf{i} \mathcal{A}_1^*.$$

In the Hopf map model, this is equivalent [10] to the constraints

$$\operatorname{Re}(\boldsymbol{\alpha}_0 \bar{\boldsymbol{\alpha}}_2 - \boldsymbol{\beta}_0 \bar{\boldsymbol{\beta}}_2) = |\boldsymbol{\alpha}_1|^2 - |\boldsymbol{\beta}_1|^2, \quad \boldsymbol{\alpha}_0 \bar{\boldsymbol{\beta}}_2 + \boldsymbol{\alpha}_2 \bar{\boldsymbol{\beta}}_0 = 2 \boldsymbol{\alpha}_1 \bar{\boldsymbol{\beta}}_1$$

on the Bernstein coefficients  $\boldsymbol{\alpha}_0, \boldsymbol{\alpha}_1, \boldsymbol{\alpha}_2$  and  $\boldsymbol{\beta}_0, \boldsymbol{\beta}_1, \boldsymbol{\beta}_2$  of  $\boldsymbol{\alpha}(t)$  and  $\boldsymbol{\beta}(t)$ .

### 3.2 Rational RMOF on DPH curves

The existence of rational RMOFs ( $\mathbf{f}, \mathbf{g}, \mathbf{b}$ ) on polynomial space curves is a more difficult problem. Whereas all PH curves have rational tangents  $\mathbf{t}(\xi)$ ,

their principal normals  $\mathbf{n}(\xi)$  and binormals  $\mathbf{b}(\xi)$  do not, in general, depend rationally on the curve parameter, because of the  $|\mathbf{r}'(\xi) \times \mathbf{r}''(\xi)|$  term in (4). To ensure a rational binormal vector, the expression

$$|\mathbf{r}' \times \mathbf{r}''|^2 = (y'z'' - y''z')^2 + (z'x'' - z''x')^2 + (x'y'' - x''y')^2$$

must be the perfect square of a polynomial in  $\xi$ . Now it can be shown [13, 15] that every PH curve satisfies the relation

$$|\mathbf{r}'(\xi) \times \mathbf{r}''(\xi)|^2 = 4\sigma^2(\xi)\rho(\xi),$$

where the polynomial  $\rho$  can be expressed in terms of  $u, v, p, q$  and  $u', v', p', q'$  in several different ways [9], the simplest being

$$\rho = (up' - u'p + vq' - v'q)^2 + (uq' - u'q - vp' + v'p)^2. \quad (20)$$

Hence, the binormal vector is rational if and only if we have

$$\rho(\xi) = \gamma^2(\xi) \quad (21)$$

for some polynomial  $\gamma(\xi)$ , i.e.,

$$|\mathbf{r}' \times \mathbf{r}''|^2 = (y'z'' - y''z')^2 + (z'x'' - z''x')^2 + (x'y'' - x''y')^2 = 4(\sigma\gamma)^2. \quad (22)$$

Polynomial curves satisfying (14) and (22) are *double PH* (DPH) curves [3, 13]. They have *rational* Frenet frames, curvature, and torsion, defined by

$$\mathbf{t} = \frac{\mathbf{r}'}{\sigma}, \quad \mathbf{p} = \frac{\sigma\mathbf{r}'' - \sigma'\mathbf{r}'}{2\sigma\gamma}, \quad \mathbf{b} = \frac{\mathbf{r}' \times \mathbf{r}''}{2\sigma\gamma}, \quad \kappa = \frac{2\gamma}{\sigma^2}, \quad \tau = \frac{(\mathbf{r}' \times \mathbf{r}'') \cdot \mathbf{r}'''}{4\sigma^2\gamma^2}. \quad (23)$$

**Remark 2.** Because of their rational Frenet frames, curvature, and torsion, we shall focus here on rational RMOFs on DPH curves, and do not address at present the existence of non-DPH curves that possess rational binormals and admit rational rotation-minimizing osculating-plane basis vectors  $\mathbf{f}, \mathbf{g}$ .

A (general) *helix* is characterized by the fact that its tangent  $\mathbf{t}$  maintains a constant inclination  $\psi$  (the *pitch* angle) with respect to a fixed direction  $\mathbf{a}$  (the *axis* of the helix) and the curvature/torsion ratio is constant [25, 32]. A *polynomial* helix must be a PH curve [15] — in fact, a DPH curve [13]. All PH cubics and all helical PH quintics are DPH curves, but non-helical DPH curves of degree  $\geq 7$  exist. Complete details may be found in [3, 13, 28].

**Remark 3.** For any DPH curve, the Frenet frame specifies a *rational pitch-free motion*, since the Frenet frame is rotation-minimizing with respect to the principal normal, and it is also rational for double PH curves.

The ERF is of no use in constructing a rational RMOF, since it does not incorporate the binormal  $\mathbf{b}$  and two rational vectors spanning the osculating plane, to which a rotation can be applied to cancel the angular velocity component in the direction of  $\mathbf{b}$ . Instead, we use the rational Frenet frame (23) for a DPH curve, and seek a rational osculating-plane rotation

$$\begin{bmatrix} \mathbf{f}(\xi) \\ \mathbf{g}(\xi) \end{bmatrix} = \frac{1}{a^2(\xi) + b^2(\xi)} \begin{bmatrix} a^2(\xi) - b^2(\xi) & -2a(\xi)b(\xi) \\ 2a(\xi)b(\xi) & a^2(\xi) - b^2(\xi) \end{bmatrix} \begin{bmatrix} \mathbf{t}(\xi) \\ \mathbf{p}(\xi) \end{bmatrix} \quad (24)$$

that maps the Frenet frame vectors  $\mathbf{t}(\xi)$ ,  $\mathbf{p}(\xi)$  to the RMOF vectors  $\mathbf{f}(\xi)$ ,  $\mathbf{g}(\xi)$  and cancels the  $\kappa \mathbf{b}$  component of the Frenet frame angular velocity (5).

Now (10) and (24) give  $\theta = -2 \tan^{-1} b/a$  and  $\theta' = 2(a'b - ab')/(a^2 + b^2)$ , and if (24) defines an RMOF, we must have  $\theta' = -\kappa \sigma$  from (11). Thus, we deduce from (23) that a DPH curve satisfying (14) and (22) has a rational RMOF if and only if polynomials  $a(\xi)$ ,  $b(\xi)$  exist, such that

$$\frac{\gamma}{u^2 + v^2 + p^2 + q^2} = \frac{ab' - a'b}{a^2 + b^2}. \quad (25)$$

### 3.3 Rational RMOF on DPH cubics

Every spatial PH cubic is a helical curve [16], and also a DPH curve [13]. Such curves admit a closed-form (but not rational) expression for the RMOF. A cubic space curve with control points  $\mathbf{p}_0, \mathbf{p}_1, \mathbf{p}_2, \mathbf{p}_3$  and control polygon leg vectors  $\mathbf{L}_0 = \mathbf{p}_1 - \mathbf{p}_0$ ,  $\mathbf{L}_1 = \mathbf{p}_2 - \mathbf{p}_1$ ,  $\mathbf{L}_2 = \mathbf{p}_3 - \mathbf{p}_2$  is a PH curve [16] if and only if  $\mathbf{L}_0, \mathbf{L}_2$  lie on a right-circular cone of half-angle  $\vartheta \leq \frac{1}{2}\pi$  about  $\mathbf{L}_1$  as axis, and their azimuthal separation  $\varphi$  on this cone is given by

$$\cos \varphi = 1 - \frac{2L_1^2}{L_0L_2}, \quad (26)$$

where  $L_i = |\mathbf{L}_i|$ . Adopting suitable coordinates, one may assume that  $\mathbf{L}_1 = L_1(0, 0, 1)$ ,  $\mathbf{L}_0 = L_0(\sin \vartheta, 0, \cos \vartheta)$ ,  $\mathbf{L}_2 = L_2(\sin \vartheta \cos \varphi \sin \vartheta \sin \varphi, \cos \vartheta)$ , with  $\varphi$  satisfying (26) and  $L_1 \leq \sqrt{L_0L_2}$ . The parametric speed is then

$$\sigma(\xi) = |\mathbf{r}'(\xi)| = 3 [L_0(1 - \xi)^2 + L_1 \cos \vartheta 2(1 - \xi)\xi + L_2\xi^2], \quad (27)$$

where  $\Delta = L_0L_2 - L_1^2 \cos^2 \vartheta \geq 0$ , so that  $\sigma(\xi) \geq 0$  for all  $\xi$ . Since  $|\mathbf{r}' \times \mathbf{r}''| = 6L_1 \sin \vartheta \sigma(\xi)$  and  $(\mathbf{r}' \times \mathbf{r}'') \cdot \mathbf{r}''' = 108 (\mathbf{L}_0 \times \mathbf{L}_1) \cdot \mathbf{L}_2$ , the curvature and torsion can be expressed [16] in terms of (27) as

$$\kappa(\xi) = \frac{6L_1 \sin \vartheta}{\sigma^2(\xi)}, \quad \tau(\xi) = \frac{-3L_0L_2 \sin \varphi}{L_1\sigma^2(\xi)}. \quad (28)$$

Hence, the angle function (11) that specifies that RMOF vectors  $\mathbf{f}, \mathbf{g}$  in terms of the Frenet frame vectors  $\mathbf{t}, \mathbf{p}$  is given by

$$\theta(\xi) = \hat{\theta}_0 - \frac{2L_1 \sin \vartheta}{\sqrt{\Delta}} \tan^{-1} \frac{(L_1 \cos \vartheta - L_0)(1 - \xi) + (L_2 - L_1 \cos \vartheta)\xi}{\sqrt{\Delta}},$$

where  $\hat{\theta}_0 = \theta_0 + (2L_1 \sin \vartheta / \sqrt{\Delta}) \tan^{-1}((L_1 \cos \vartheta - L_0) / \sqrt{\Delta})$ .

**Proposition 2.** *The condition (25) for a rational RMOF can be satisfied by PH cubics only in the degenerate case of planar curves.*

**Proof :** Since  $|\mathbf{r}' \times \mathbf{r}''|^2 = 4(\sigma\gamma)^2$  and  $|\mathbf{r}' \times \mathbf{r}''| = 6L_1 \sin \vartheta \sigma$  we see that  $\gamma(\xi) = 3L_1 \sin \vartheta$  is a constant. Substituting this together with (27) for the denominator on the left in (25), and assuming  $a(\xi) = a_0(1 - \xi) + a_1\xi$ ,  $b(\xi) = b_0(1 - \xi) + b_1\xi$  on the right, satisfaction of (25) requires that

$$a_0b_1 - a_1b_0 = 3L_1 \sin \vartheta, \quad a_0^2 + b_0^2 = 3L_0, \quad a_0a_1 + b_0b_1 = 3L_1 \cos \vartheta, \quad a_1^2 + b_1^2 = 3L_2.$$

With  $\mathbf{c}_0 = a_0 + i b_0$ ,  $\mathbf{c}_1 = a_1 + i b_1$  these equations are equivalent to  $|\mathbf{c}_0|^2 = 3L_0$ ,  $\bar{\mathbf{c}}_0\mathbf{c}_1 = 3L_1 e^{i\vartheta}$ ,  $|\mathbf{c}_1|^2 = 3L_2$ , and we must have  $|\mathbf{c}_0| = \sqrt{3L_0}$ ,  $|\mathbf{c}_0| |\mathbf{c}_1| = 3L_1$ ,  $|\mathbf{c}_1| = \sqrt{3L_2}$ . From (26) these conditions imply that  $\cos \varphi = -1$ ,  $\sin \varphi = 0$ . It then follows from (28) that the torsion vanishes, so the curve is planar. ■

### 3.4 Rational RMOF on DPH quintics

One is thus led to consider satisfaction of (25) in the case of DPH quintics, which are equivalent to the quintic helical polynomial space curves: for such curves,  $\gamma(\xi)$  is a quadratic polynomial. The characterization of curves that have rational RMOFs, as solutions to (25), is more difficult than the problem of identifying curves with rational RMAFs, satisfying (19). Unlike (19), the numerator polynomial on the left in (25) is not known explicitly in terms of  $u, v, p, q$  — instead,  $\gamma$  must be determined from conditions (20)–(21).

Now for the polynomials (17) defining the Hopf map form (18), we have

$$\boldsymbol{\alpha}\boldsymbol{\beta}' - \boldsymbol{\alpha}'\boldsymbol{\beta} = (uq' - u'q - vp' + v'p) + i(up' - u'p + vq' - v'q),$$

and hence (20) can be written as  $\rho = |\boldsymbol{\alpha}\boldsymbol{\beta}' - \boldsymbol{\alpha}'\boldsymbol{\beta}|^2$ . The condition (21) for  $\rho$  to be a perfect square is thus equivalent [13, 28] to the requirement that

$$\boldsymbol{\alpha}(\xi)\boldsymbol{\beta}'(\xi) - \boldsymbol{\alpha}'(\xi)\boldsymbol{\beta}(\xi) = h(\xi)\mathbf{w}^2(\xi) \quad (29)$$

for a real polynomial  $h(\xi)$  and complex polynomial  $\mathbf{w}(\xi) = r(\xi) + i s(\xi)$  with  $\gcd(r(\xi), s(\xi)) = 1$ , where  $\deg(h) + 2\deg(\mathbf{w}) = 2\max(\deg(\boldsymbol{\alpha}), \deg(\boldsymbol{\beta})) - 2$ . The polynomial  $\gamma(\xi)$  defined by (21) is then given by  $\gamma(\xi) = h(\xi)|\mathbf{w}(\xi)|^2$ .

For DPH quintics with  $\max(\deg(\boldsymbol{\alpha}), \deg(\boldsymbol{\beta})) = 2$ , the solutions to (29) may be categorized according to whether (a)  $\deg(h) = 0$  and  $\deg(\mathbf{w}) = 1$ ; or (b)  $\deg(h) = 2$  and  $\deg(\mathbf{w}) = 0$ . These correspond [3, 13, 15, 28] to the *monotone helical* and *general helical* PH quintics, respectively — the former maintain a fixed sense of rotation of the tangent  $\mathbf{t}$  about the axis  $\mathbf{a}$ , while the latter may exhibit a reversal of the sense of rotation.

In case (a) we may set  $h(\xi) = 1$  and  $\mathbf{w}(\xi) = \mathbf{w}_0(1 - \xi) + \mathbf{w}_1\xi$  without loss of generality. Satisfaction of (29) by quadratic polynomials  $\boldsymbol{\alpha}(t)$  and  $\boldsymbol{\beta}(t)$  with Bernstein coefficients  $\boldsymbol{\alpha}_0, \boldsymbol{\alpha}_1, \boldsymbol{\alpha}_2$  and  $\boldsymbol{\beta}_0, \boldsymbol{\beta}_1, \boldsymbol{\beta}_2$  then implies that

$$(\boldsymbol{\alpha}_0\boldsymbol{\beta}_1 - \boldsymbol{\alpha}_1\boldsymbol{\beta}_0, \boldsymbol{\alpha}_0\boldsymbol{\beta}_2 - \boldsymbol{\alpha}_2\boldsymbol{\beta}_0, \boldsymbol{\alpha}_1\boldsymbol{\beta}_2 - \boldsymbol{\alpha}_2\boldsymbol{\beta}_1) = (\frac{1}{2}\mathbf{w}_0^2, \mathbf{w}_0\mathbf{w}_1, \frac{1}{2}\mathbf{w}_1^2) \quad (30)$$

which is equivalent to  $(\boldsymbol{\alpha}_0\boldsymbol{\beta}_1 - \boldsymbol{\alpha}_1\boldsymbol{\beta}_0)(\boldsymbol{\alpha}_1\boldsymbol{\beta}_2 - \boldsymbol{\alpha}_2\boldsymbol{\beta}_1) = \frac{1}{4}(\boldsymbol{\alpha}_0\boldsymbol{\beta}_2 - \boldsymbol{\alpha}_2\boldsymbol{\beta}_0)^2$ . If this constraint is satisfied and  $\mathbf{w}_0, \mathbf{w}_1$  are complex values determined from (30), the polynomial  $\gamma(\xi)$  in the rational RMOF condition (25) has the form

$$\gamma(\xi) = |\mathbf{w}_0|^2(1 - \xi)^2 + \operatorname{Re}(\overline{\mathbf{w}_0}\mathbf{w}_1)2(1 - \xi)\xi + |\mathbf{w}_1|^2\xi^2.$$

In case (b) we set  $h(\xi) = h_0(1 - \xi)^2 + h_12(1 - \xi)\xi + h_2\xi^2$  and  $\mathbf{w}(\xi) = e^{i\zeta}$  without loss of generality. Then satisfaction of (29) implies that

$$(\boldsymbol{\alpha}_0\boldsymbol{\beta}_1 - \boldsymbol{\alpha}_1\boldsymbol{\beta}_0, \boldsymbol{\alpha}_0\boldsymbol{\beta}_2 - \boldsymbol{\alpha}_2\boldsymbol{\beta}_0, \boldsymbol{\alpha}_1\boldsymbol{\beta}_2 - \boldsymbol{\alpha}_2\boldsymbol{\beta}_1) = (\frac{1}{2}h_0e^{i2\zeta}, h_1e^{i2\zeta}, \frac{1}{2}h_2e^{i\zeta}) \quad (31)$$

i.e.,  $\boldsymbol{\alpha}_0\boldsymbol{\beta}_1 - \boldsymbol{\alpha}_1\boldsymbol{\beta}_0, \boldsymbol{\alpha}_0\boldsymbol{\beta}_2 - \boldsymbol{\alpha}_2\boldsymbol{\beta}_0, \boldsymbol{\alpha}_1\boldsymbol{\beta}_2 - \boldsymbol{\alpha}_2\boldsymbol{\beta}_1$  are just real multiples of each other. In this case, with the coefficients of  $\boldsymbol{\alpha}(t)$  and  $\boldsymbol{\beta}(t)$  satisfying (31), the polynomial  $\gamma(\xi)$  in (25) has the form  $\gamma(\xi) = h_0(1 - \xi)^2 + h_12(1 - \xi)\xi + h_2\xi^2$ .

Equations (30) and (31) differ only in the complex values on the right. We now consider their solutions for general values  $(\mathbf{z}_0, \mathbf{z}_1, \mathbf{z}_2) \neq (0, 0, 0)$  on the right, focusing on the “generic” case with  $\mathbf{z}_1 \neq 0$  and  $\mathbf{z}_0\boldsymbol{\alpha}_2 + \mathbf{z}_2\boldsymbol{\alpha}_0 \neq 0$  (the cases  $\mathbf{z}_1 = 0$  or  $\mathbf{z}_0\boldsymbol{\alpha}_2 + \mathbf{z}_2\boldsymbol{\alpha}_0 = 0$  also yield only linear or planar curves: since the arguments for these cases are rather technical, we omit them).



**Remark 4.** If  $(\mathbf{z}_0, \mathbf{z}_1, \mathbf{z}_2) = (0, 0, 0)$  the left-hand side of (25) vanishes, and it is satisfied with  $a(\xi), b(\xi)$  constant, i.e., the Frenet frame is an RMOF. But this occurs only if the curvature vanishes, so the curve is just a straight line.

**Proposition 3.** For  $\mathbf{z}_1 \neq 0$ , the solutions to the system of equations

$$\alpha_0\beta_1 - \alpha_1\beta_0 = \mathbf{z}_0, \quad \alpha_0\beta_2 - \alpha_2\beta_0 = \mathbf{z}_1, \quad \alpha_1\beta_2 - \alpha_2\beta_1 = \mathbf{z}_2, \quad (32)$$

where  $\mathbf{z}_0\alpha_2 + \mathbf{z}_2\alpha_0 \neq 0$  may be defined by expressing  $\alpha_1, \beta_0, \beta_2$  in terms of  $\alpha_0, \alpha_2, \beta_1$  as

$$\alpha_1 = \frac{\mathbf{z}_0\alpha_2 + \mathbf{z}_2\alpha_0}{\mathbf{z}_1}, \quad \beta_0 = \frac{(\alpha_0\beta_1 - \mathbf{z}_0)\mathbf{z}_1}{\mathbf{z}_0\alpha_2 + \mathbf{z}_2\alpha_0}, \quad \beta_2 = \frac{(\alpha_2\beta_1 + \mathbf{z}_2)\mathbf{z}_1}{\mathbf{z}_0\alpha_2 + \mathbf{z}_2\alpha_0}. \quad (33)$$

**Proof :** Writing (32) as a linear system for  $\beta_0, \beta_1, \beta_2$  in the form

$$\begin{bmatrix} -\alpha_1 & \alpha_0 & 0 \\ -\alpha_2 & 0 & \alpha_0 \\ 0 & -\alpha_2 & \alpha_1 \end{bmatrix} \begin{bmatrix} \beta_0 \\ \beta_1 \\ \beta_2 \end{bmatrix} = \begin{bmatrix} \mathbf{z}_0 \\ \mathbf{z}_1 \\ \mathbf{z}_2 \end{bmatrix}, \quad (34)$$

the matrix on the left is seen to be of rank 2. Solutions exist if and only if the  $3 \times 4$  augmented matrix, defined by appending the vector on the right in (34) as a fourth column to the matrix on the left, is also of rank 2. The determinants of the three  $3 \times 3$  matrices defined by combining two of the first three columns of the augmented matrix with the last column are

$$\alpha_2(\mathbf{z}_0\alpha_2 + \mathbf{z}_2\alpha_0 - \mathbf{z}_1\alpha_1), \quad -\alpha_1(\mathbf{z}_0\alpha_2 + \mathbf{z}_2\alpha_0 - \mathbf{z}_1\alpha_1), \quad \alpha_0(\mathbf{z}_0\alpha_2 + \mathbf{z}_2\alpha_0 - \mathbf{z}_1\alpha_1).$$

Now  $(\alpha_0, \alpha_1, \alpha_2) = (0, 0, 0)$  cannot satisfy (32) if  $\mathbf{z}_1 \neq 0$ , so we must have

$$\mathbf{z}_0\alpha_2 + \mathbf{z}_2\alpha_0 - \mathbf{z}_1\alpha_1 = 0.$$

This condition yields the expression for  $\alpha_1$  in (33) and if it holds, equations (34) admit solutions in which one of  $\beta_0, \beta_1, \beta_2$  may be treated as a parameter. Choosing  $\beta_1$  as the free parameter, and substituting for  $\alpha_1$  into the first and third of equations (32), we obtain the expressions for  $\beta_0, \beta_2$  in (33). ■

Hence, when equations (32) are satisfied with  $\mathbf{z}_1 \neq 0$  and  $\mathbf{z}_0\alpha_2 + \mathbf{z}_2\alpha_0 \neq 0$ , we can express  $\alpha(t), \beta(t)$  in terms of  $\alpha_0, \alpha_2, \beta_1$  and  $\mathbf{z}_0, \mathbf{z}_1, \mathbf{z}_2$  as

$$\alpha(\xi) = \alpha_0(1 - \xi)^2 + \frac{\mathbf{z}_0\alpha_2 + \mathbf{z}_2\alpha_0}{\mathbf{z}_1} 2(1 - \xi)\xi + \alpha_2\xi^2,$$

$$\boldsymbol{\beta}(\xi) = \frac{(\boldsymbol{\alpha}_0 \boldsymbol{\beta}_1 - \mathbf{z}_0) \mathbf{z}_1}{\mathbf{z}_0 \boldsymbol{\alpha}_2 + \mathbf{z}_2 \boldsymbol{\alpha}_0} (1 - \xi)^2 + \boldsymbol{\beta}_1 2(1 - \xi)\xi + \frac{(\boldsymbol{\alpha}_2 \boldsymbol{\beta}_1 + \mathbf{z}_2) \mathbf{z}_1}{\mathbf{z}_0 \boldsymbol{\alpha}_2 + \mathbf{z}_2 \boldsymbol{\alpha}_0} \xi^2.$$

Considerable simplification is achieved by considering *canonical form* curves, with  $(\boldsymbol{\alpha}_0, \boldsymbol{\beta}_0) = (1, 0)$ . Since canonical form is achieved by a scaling/rotation, that maps  $\mathbf{r}'(0)$  to the unit vector  $\mathbf{i}$ , it does not alter the PH or DPH nature of a curve, or the existence of rational rotation–minimizing frames on it [10].

Setting  $\boldsymbol{\alpha}_0 = 1$  and  $\boldsymbol{\beta}_1 = \mathbf{z}_0$  gives the canonical–form polynomials

$$\begin{aligned} \boldsymbol{\alpha}(\xi) &= (1 - \xi)^2 + \frac{\mathbf{z}_0 \boldsymbol{\alpha}_2 + \mathbf{z}_2}{\mathbf{z}_1} 2(1 - \xi)\xi + \boldsymbol{\alpha}_2 \xi^2, \\ \boldsymbol{\beta}(\xi) &= \mathbf{z}_0 2(1 - \xi)\xi + \mathbf{z}_1 \xi^2. \end{aligned} \quad (35)$$

These polynomials define a monotone or general helical DPH quintic, when  $(\mathbf{z}_0, \mathbf{z}_1, \mathbf{z}_2)$  are of the form  $(\frac{1}{2}\mathbf{w}_0^2, \mathbf{w}_0 \mathbf{w}_1, \frac{1}{2}\mathbf{w}_1^2)$  or  $e^{i2\zeta}(\frac{1}{2}h_0, h_1, \frac{1}{2}h_2)$ .

Now suppose that condition (25) is satisfied with quadratic polynomials  $a(\xi)$ ,  $b(\xi)$ . Combining them into a complex polynomial  $\mathbf{c}(\xi) = a(\xi) + i b(\xi)$  with Bernstein coefficients  $\mathbf{c}_0$ ,  $\mathbf{c}_1$ ,  $\mathbf{c}_2$ , we see that the right–hand side of (25) is equal to  $\text{Im}(\overline{\mathbf{c}}\mathbf{c}')/|\mathbf{c}|^2$ . Since this expression is unchanged on dividing  $\mathbf{c}(\xi)$  by any complex constant, we may choose  $\mathbf{c}_0 = 1$  without loss of generality.

With  $\mathbf{c}_0 = 1$ , if  $\gamma_0, \gamma_1, \gamma_2$  are the Bernstein coefficients of  $\gamma(\xi)$ , satisfaction of (25) means that for some real number  $\ell \neq 0$  we must have

$$\gamma_0 = 2\ell \text{Im}(\mathbf{c}_1), \quad \gamma_1 = \ell \text{Im}(\mathbf{c}_2), \quad \gamma_2 = 2\ell \text{Im}(\overline{\mathbf{c}}_1 \mathbf{c}_2), \quad (36)$$

$$\begin{aligned} |\boldsymbol{\alpha}_0|^2 + |\boldsymbol{\beta}_0|^2 &= \ell, \\ \text{Re}(\boldsymbol{\alpha}_0 \overline{\boldsymbol{\alpha}}_1 + \boldsymbol{\beta}_0 \overline{\boldsymbol{\beta}}_1) &= \ell \text{Re}(\overline{\mathbf{c}}_1), \\ \text{Re}(\overline{\boldsymbol{\alpha}}_0 \boldsymbol{\alpha}_2 + \overline{\boldsymbol{\beta}}_0 \boldsymbol{\beta}_2) + 2(|\boldsymbol{\alpha}_1|^2 + |\boldsymbol{\beta}_1|^2) &= \ell (\text{Re}(\overline{\mathbf{c}}_2) + 2|\mathbf{c}_1|^2), \\ \text{Re}(\boldsymbol{\alpha}_1 \overline{\boldsymbol{\alpha}}_2 + \boldsymbol{\beta}_1 \overline{\boldsymbol{\beta}}_2) &= \ell \text{Re}(\mathbf{c}_1 \overline{\mathbf{c}}_2), \\ |\boldsymbol{\alpha}_2|^2 + |\boldsymbol{\beta}_2|^2 &= \ell |\mathbf{c}_2|^2. \end{aligned} \quad (37)$$

### 3.4.1 Monotone helical quintics

For the DPH quintic specified by (35) with  $(\mathbf{z}_0, \mathbf{z}_1, \mathbf{z}_2) = (\frac{1}{2}\mathbf{w}_0^2, \mathbf{w}_0 \mathbf{w}_1, \frac{1}{2}\mathbf{w}_1^2)$  and  $(\gamma_0, \gamma_1, \gamma_2) = (|\mathbf{w}_0|^2, \text{Re}(\mathbf{w}_0 \overline{\mathbf{w}}_1), |\mathbf{w}_1|^2)$ , we obtain  $\ell = 1$  from the first

equation in (37). Equations (36) and the other equations in (37) are then

$$|\mathbf{w}_0|^2 = 2 \operatorname{Im}(\mathbf{c}_1), \quad \operatorname{Re}(\overline{\mathbf{w}}_0 \mathbf{w}_1) = \operatorname{Im}(\mathbf{c}_2), \quad |\mathbf{w}_1|^2 = 2 \operatorname{Im}(\overline{\mathbf{c}}_1 \mathbf{c}_2),$$

$$\operatorname{Re}(\overline{\boldsymbol{\alpha}}_1) = \operatorname{Re}(\overline{\mathbf{c}}_1),$$

$$\operatorname{Re}(\boldsymbol{\alpha}_2) + 2|\boldsymbol{\alpha}_1|^2 + \frac{1}{2}|\mathbf{w}_0|^4 = \operatorname{Re}(\overline{\mathbf{c}}_2) + 2|\mathbf{c}_1|^2,$$

$$\operatorname{Re}(\boldsymbol{\alpha}_1 \overline{\boldsymbol{\alpha}}_2 + \frac{1}{2}|\mathbf{w}_0|^2 \mathbf{w}_0 \overline{\mathbf{w}}_1) = \operatorname{Re}(\mathbf{c}_1 \overline{\mathbf{c}}_2),$$

$$|\boldsymbol{\alpha}_2|^2 + |\mathbf{w}_0|^2 |\mathbf{w}_1|^2 = |\mathbf{c}_2|^2,$$

where  $\boldsymbol{\alpha}_1 = \frac{1}{2}(\mathbf{w}_1/\mathbf{w}_0) + \frac{1}{2}(\mathbf{w}_0/\mathbf{w}_1)\boldsymbol{\alpha}_2$ ,  $\boldsymbol{\alpha}_2$  is free, and  $\boldsymbol{\beta}_1 = \frac{1}{2}\mathbf{w}_0^2$ ,  $\boldsymbol{\beta}_2 = \mathbf{w}_0 \mathbf{w}_1$ . Setting  $\mathbf{c}_1 = a_1 + i b_1$ ,  $\mathbf{c}_2 = a_2 + i b_2$ ,  $\mathbf{w}_0 = w_0 e^{i\phi_0}$ ,  $\mathbf{w}_1 = w_1 e^{i\phi_1}$ ,  $\boldsymbol{\alpha}_2 = u_2 + i v_2$ ,  $c = \cos(\phi_1 - \phi_0)$ ,  $s = \sin(\phi_1 - \phi_0)$  then gives

$$w_0^2 = 2b_1, \quad w_0 w_1 c = b_2, \quad w_1^2 = 2(a_1 b_2 - a_2 b_1), \quad (38)$$

$$\frac{w_0}{w_1}(c u_2 + s v_2) + \frac{w_1}{w_0} c = 2a_1,$$

$$4c(c u_2 + s v_2) + \frac{w_0^2}{w_1^2}(u_2^2 + v_2^2) + \frac{w_1^2}{w_0^2} + w_0^4 = 2a_2 + 4(a_1^2 + b_1^2), \quad (39)$$

$$\frac{w_1}{w_0}(c u_2 + s v_2) + \frac{w_0}{w_1} c (u_2^2 + v_2^2) + w_0^3 w_1 c = 2(a_1 a_2 + b_1 b_2),$$

$$u_2^2 + v_2^2 + w_0^2 w_1^2 = a_2^2 + b_2^2.$$

**Lemma 2.** *The solutions to (38)–(39) generate straight lines if  $b_1 = 0$ , and planar curves if  $v_2 = 0$  and  $\phi_1 = \phi_0 + k\pi$  for integer  $k$ , i.e.,  $(c, s) = (\pm 1, 0)$ .*

**Proof:** If  $b_1 = 0$ , equations (38) imply that  $w_0 = w_1 = 0$ , and thus  $\mathbf{w}(\xi) \equiv 0$ . Consequently, from (29) we have  $\boldsymbol{\alpha}(\xi)\boldsymbol{\beta}'(\xi) - \boldsymbol{\alpha}'(\xi)\boldsymbol{\beta}(\xi) \equiv 0$ , and since the curvature of  $\mathbf{r}(\xi)$  can be expressed [13] as

$$\kappa(\xi) = 2 \frac{|\boldsymbol{\alpha}(\xi)\boldsymbol{\beta}'(\xi) - \boldsymbol{\alpha}'(\xi)\boldsymbol{\beta}(\xi)|}{(|\boldsymbol{\alpha}(\xi)|^2 + |\boldsymbol{\beta}(\xi)|^2)^2},$$

this implies that  $\kappa(\xi) \equiv 0$  — i.e., the curve degenerates to a straight line. If  $\phi_1 = \phi_0 + k\pi$  and  $v_2 = 0$  (i.e.,  $\boldsymbol{\alpha}_2$  is real), we have

$$(\boldsymbol{\alpha}_0, \boldsymbol{\alpha}_1, \boldsymbol{\alpha}_2) = (1, \pm \frac{1}{2}[(w_1/w_0) + (w_0/w_1)u_2], u_2),$$

$$(\boldsymbol{\beta}_0, \boldsymbol{\beta}_1, \boldsymbol{\beta}_2) = e^{i^2\phi_0} (0, \frac{1}{2}w_0^2, \pm w_0w_1),$$

and  $\boldsymbol{\alpha}(\xi), \boldsymbol{\beta}(\xi)$  are thus of the form stated in Lemma 1 for a planar curve. ■

**Proposition 4.** *Monotone helical DPH quintics admit rational RMOFs only in the degenerate cases of straight lines or planar curves.*

**Proof :** For equations (38) to define real  $w_0, w_1$  values we must have  $b_1 > 0$  and  $a_1b_2 - a_2b_1 \geq 0$ , where we invoke Lemma 2 to discount the case  $b_1 = 0$ . Moreover, consistency of these equations implies that

$$c^2 = \frac{b_2^2}{4(a_1b_2 - a_2b_1)b_1}, \quad (40)$$

and hence we must also have  $4(a_1b_2 - a_2b_1)b_1 \geq b_2^2$ . Assuming these conditions hold, substituting (38) and (40) into (39) gives

$$4\frac{b_1}{b_2}c(cu_2 + sv_2) + \frac{b_2}{b_1} = 4a_1,$$

$$4c(cu_2 + sv_2) + \frac{b_1}{a_1b_2 - a_2b_1}(u_2^2 + v_2^2) + \frac{a_1b_2 - a_2b_1}{b_1} = 2a_2 + 4a_1^2,$$

$$4\frac{a_1b_2 - a_2b_1}{b_2}c(cu_2 + sv_2) + \frac{b_2}{a_1b_2 - a_2b_1}(u_2^2 + v_2^2) = 4a_1a_2,$$

$$u_2^2 + v_2^2 + 4(a_1b_2 - a_2b_1)b_1 = a_2^2 + b_2^2.$$

From the first and fourth of these equations we obtain

$$c(cu_2 + sv_2) = \frac{b_2}{b_1} \left( a_1 - \frac{b_2}{4b_1} \right), \quad u_2^2 + v_2^2 = a_2^2 + b_2^2 - 4(a_1b_2 - a_2b_1)b_1, \quad (41)$$

and thus, to ensure that  $\boldsymbol{\alpha}_2 = u_2 + i v_2$  exists, we have the further inequality  $a_2^2 + b_2^2 \geq 4(a_1b_2 - a_2b_1)b_1$ . On substituting (41) into the second and third equations, we arrive at two conditions involving only  $a_1, b_1, a_2, b_2$  — namely

$$\left[ \frac{a_1^2 + b_1^2}{a_1b_2 - a_2b_1} - \frac{1}{b_1} \right] \left[ \frac{b_2^2}{b_1} - 4(a_1b_2 - a_2b_1) \right] = 0, \quad (42)$$

$$\left[ \frac{a_1 a_2 + b_1 b_2}{a_1 b_2 - a_2 b_1} - \frac{a_1}{b_1} \right] \left[ \frac{b_2^2}{b_1} - 4(a_1 b_2 - a_2 b_1) \right] = 0. \quad (43)$$

Consider first the case where the common second factor in (42)–(43) vanishes. Then  $(c, s) = (\pm 1, 0)$  from (40), and equations (41) reduce to

$$u_2 = \frac{b_2}{b_1} \left( a_1 - \frac{b_2}{4b_1} \right), \quad u_2^2 + v_2^2 = a_2^2.$$

Substituting the former into the latter gives

$$v_2^2 = \frac{[b_2^2 - 4(a_1 b_2 - a_2 b_1)b_1][4(a_1 b_2 + a_2 b_1)b_1 - b_2^2]}{16 b_1^4},$$

and since  $b_2^2 - 4(a_1 b_2 - a_2 b_1)b_1 = 0$ , we obtain  $v_2 = 0$ . The conditions  $v_2 = 0$  and  $(c, s) = (\pm 1, 0)$  of Lemma 2 for a planar curve are thus satisfied.

Now consider that case where the first factors in equations (42)–(43) vanish simultaneously. This occurs (provided that  $a_1^2 \geq a_2$ ) when

$$b_1 = \pm \sqrt{a_1^2 - a_2} \quad \text{and} \quad b_2 = \pm 2 a_1 \sqrt{a_1^2 - a_2}. \quad (44)$$

From (40) we then have  $c^2 = a_1^2 / (2 a_1^2 - a_2)$ , and using this together with  $s^2 = 1 - c^2$  in (41) gives  $v_2^2 = a_1^2 (2 a_1^2 - a_2 - u_2)^2 / (a_1^2 - a_2)$ . Substituting into the second of equations (41) and simplifying yields the quadratic equation

$$u_2^2 - 2 a_1^2 u_2 + 4 a_1^4 - 6 a_1^2 a_2 + 3 a_2^2 = 0$$

in  $u_2$ . Since this has discriminant  $-12(a_1^2 - a_2)^2$ , there are no real solutions for  $u_2$  unless  $a_1^2 = a_2$ , in which case we have  $b_1 = 0$  from (44) and Lemma 2 implies that the curve degenerates into a straight line. ■

### 3.4.2 General helical quintics

For a DPH quintic specified by (35) with  $(\mathbf{z}_0, \mathbf{z}_1, \mathbf{z}_2) = (\frac{1}{2}h_0 e^{i2\zeta}, h_1 e^{i2\zeta}, \frac{1}{2}h_2 e^{i2\zeta})$  and  $(\gamma_0, \gamma_1, \gamma_2) = (h_0, h_1, h_2)$ , we have  $\ell = 1$  again from the first equation in (37), so (36) and the other equations in (37) become

$$h_0 = 2 \operatorname{Im}(\mathbf{c}_1), \quad h_1 = \operatorname{Im}(\mathbf{c}_2), \quad h_2 = 2 \operatorname{Im}(\bar{\mathbf{c}}_1 \mathbf{c}_2),$$

$$\operatorname{Re}(\bar{\boldsymbol{\alpha}}_1) = \operatorname{Re}(\bar{\mathbf{c}}_1),$$

$$\operatorname{Re}(\boldsymbol{\alpha}_2) + 2(|\boldsymbol{\alpha}_1|^2 + |\boldsymbol{\beta}_1|^2) = \operatorname{Re}(\bar{\mathbf{c}}_2) + 2|b f c_1|^2,$$

$$\operatorname{Re}(\boldsymbol{\alpha}_1 \bar{\boldsymbol{\alpha}}_2 + \boldsymbol{\beta}_1 \bar{\boldsymbol{\beta}}_2) = \operatorname{Re}(\mathbf{c}_1 \bar{\mathbf{c}}_2),$$

$$|\boldsymbol{\alpha}_2|^2 + |\boldsymbol{\beta}_2|^2 = |\mathbf{c}_2|^2,$$

with  $\alpha_1 = \frac{1}{2}(h_0\alpha_2 + h_2)/h_1$ ,  $\alpha_2$  free, and  $\beta_1 = \frac{1}{2}h_0e^{i2\zeta}$ ,  $\beta_2 = h_1e^{i2\zeta}$ . Setting  $c_1 = a_1 + ib_1$ ,  $c_2 = a_2 + ib_2$ ,  $\alpha_2 = u_2 + iv_2$  then gives

$$h_0 = 2b_1, \quad h_1 = b_2, \quad h_2 = 2(a_1b_2 - a_2b_1), \quad (45)$$

$$\begin{aligned} h_0u_2 + h_2 &= 2h_1a_1, \\ 2(h_1^2 + h_0h_2)u_2 + h_0^2(u_2^2 + v_2^2) + h_0^2h_1^2 + h_2^2 &= 2h_1^2[a_2 + 2(a_1^2 + b_1^2)], \\ h_0(u_2^2 + v_2^2) + h_2u_2 + h_0h_1^2 &= 2h_1(a_1a_2 + b_1b_2), \\ u_2^2 + v_2^2 + h_1^2 &= a_2^2 + b_2^2. \end{aligned} \quad (46)$$

**Proposition 5.** *General helical DPH quintics admit rational RMOFs only in the degenerate case of planar curves.*

**Proof :** Substituting (45) into (46) and simplifying gives

$$\begin{aligned} u_2 &= a_2, \\ (b_2^2 + 4(a_1b_2 - a_2b_1)b_1)u_2 + 2b_1^2(u_2^2 + v_2^2) &= 4a_1a_2b_1b_2 + a_2b_2^2 - 2a_2^2b_1^2, \\ b_1(u_2^2 + v_2^2) + (a_1b_2 - a_2b_1)u_2 &= a_1a_2b_2, \\ u_2^2 + v_2^2 &= a_2^2. \end{aligned}$$

From the first and fourth equations we have  $(u_2, v_2) = (a_2, 0)$  and these values also satisfy the other equations. Hence,  $\alpha_2 = u_2$  and  $\alpha_1 = \frac{1}{2}(h_0u_2 + h_2)/h_1$ , and  $\alpha(\xi)$ ,  $\beta(\xi)$  have the form identified in Lemma 1 with planar curves, since  $(\alpha_0, \alpha_1, \alpha_2) = (1, \frac{1}{2}(h_0u_2 + h_2)/h_1, u_2)$  and  $(\beta_0, \beta_1, \beta_2) = e^{i2\psi}(0, \frac{1}{2}h_0, h_1)$ . ■

## 4 Ruled surfaces

Surfaces generated by the motion of a straight line through space are called *ruled surfaces*. Each instance of the line is a *ruling* or *generator* of the surface. A special class of ruled surfaces, the *developable surfaces*, is characterized by a constant surface normal along each ruling. A surface is developable if and only if it is the envelope of a one-parameter family of planes. A developable surface, regarded as a thin material sheet, can be “flattened” (or *developed*) onto a plane, without stretching or compressing it [22, 25, 32].

Several important ruled surfaces are associated with a space curve. The surface generated by the curve tangent lines is a developable surface, known

as the *tangent developable* — it can also be interpreted as the envelope of the curve osculating planes. However, for space curves, the surfaces generated by lines along the principal normal and binormal directions at each point are not developable [25]. The envelopes of the normal planes and the rectifying planes to a space curve are called the *polar developable* and *rectifying developable*.

If the tangent developable is developed onto a plane, the space curve maps to a plane curve, the generators of the surface becoming its tangents. The two curves have equal curvatures at corresponding points, and equal arc lengths of corresponding segments [22]. When the rectifying developable is developed onto a plane, the curve maps to a straight line, corresponding segments of the curve and the line having equal lengths. The polar developable can be regarded as the analog, for a space curve, of the *evolute* of a plane curve [32].

Consider the construction of a ruled surface from a space curve  $\mathbf{r}(\xi)$ , such that the surface tangent plane is coincident with the curve osculating plane. Expressing the surface in terms of a unit vector  $\mathbf{d}(\xi)$  defined along  $\mathbf{r}(\xi)$  as

$$\mathbf{s}(\xi, \lambda) = \mathbf{r}(\xi) + \lambda \mathbf{d}(\xi), \quad (47)$$

it has the desired property if  $\mathbf{d}(\xi)$  is of the form

$$\mathbf{d}(\xi) = \cos \Theta(\xi) \mathbf{t}(\xi) + \sin \Theta(\xi) \mathbf{p}(\xi) \quad (48)$$

since we then have

$$\mathbf{s}_\xi \times \mathbf{s}_\lambda = \sin \Theta \sigma \mathbf{b} + \lambda [\sin \Theta \sigma \tau (\cos \Theta \mathbf{p} - \sin \Theta \mathbf{t}) - (\Theta' + \sigma \kappa) \mathbf{b}],$$

and thus when  $\lambda = 0$  — i.e., along the curve  $\mathbf{r}(\xi)$  — the surface normal is

$$\mathbf{n} = \frac{\mathbf{s}_\xi \times \mathbf{s}_\lambda}{|\mathbf{s}_\xi \times \mathbf{s}_\lambda|} = -\text{sign}(\sin \Theta) \mathbf{b}. \quad (49)$$

Coincidence of the osculating plane of  $\mathbf{r}(\xi)$  with the tangent plane of  $\mathbf{s}(\xi, \lambda)$  identifies the curve as an *asymptotic line* of the surface (47).

The tangent developable and the principal normal surface correspond to choosing  $\mathbf{t}(\xi)$  and  $\mathbf{p}(\xi)$  for  $\mathbf{d}(\xi)$ . The angular velocity describing the changing orientation of the rulings in these cases is the Darboux vector,  $\boldsymbol{\omega} = \kappa \mathbf{b} + \tau \mathbf{t}$ . However, the component  $\kappa \mathbf{b}$  of this angular velocity defines an orientational change within the osculating plane, that is “unnecessary” to satisfaction of the constraints imposed on  $\mathbf{s}(\xi, \lambda)$ . A ruled surface satisfying the prescribed interpolation conditions, with the least orientational variation of its rulings, can be constructed by choosing one of the RMOF vectors  $\mathbf{f}(\xi)$ ,  $\mathbf{g}(\xi)$  defined by (10)–(11) — or any vector fixed relative to them — for  $\mathbf{d}(\xi)$ .

## 4.1 Tangent developable

The family of tangent lines to a curve  $\mathbf{r}(\xi)$  define the ruled surface

$$\mathbf{s}(\xi, \lambda) = \mathbf{r}(\xi) + \lambda \mathbf{t}(\xi), \quad (50)$$

with derivatives  $\mathbf{s}_\xi = \sigma(\mathbf{t} + \lambda\kappa\mathbf{p})$  and  $\mathbf{s}_\lambda = \mathbf{t}$  satisfying  $\mathbf{s}_\xi \times \mathbf{s}_\lambda = -\sigma\lambda\kappa\mathbf{b}$ . Thus, if  $\mathbf{r}(\xi)$  is regular with non-vanishing curvature, the surface normal is

$$\mathbf{n} = \frac{\mathbf{s}_\xi \times \mathbf{s}_\lambda}{|\mathbf{s}_\xi \times \mathbf{s}_\lambda|} = -\text{sign}(\lambda)\mathbf{b}.$$

This is the singular case  $\Theta(\xi) \equiv 0$  of (49). The tangent developable consists of two “sheets” corresponding to  $\lambda < 0$  and  $\lambda > 0$  that meet at  $\lambda = 0$ , i.e., along the curve  $\mathbf{r}(\xi)$ , where  $\mathbf{n}$  is indeterminate (it is also indeterminate along rulings corresponding to points at which  $\kappa = 0$  — i.e., the *inflections* of  $\mathbf{r}(\xi)$ ). Since  $\mathbf{n}$  exhibits a sudden reversal on passing through  $\lambda = 0$  along a ruling of the surface (50), the curve  $\mathbf{r}(\xi)$  is called [25] the *cuspidal edge* or *edge of regression* of the tangent surface  $\mathbf{s}(\xi, \lambda)$ . It may also be regarded as the locus of intersection points of neighboring generators, at parameter values  $\xi$  and  $\xi + \delta\xi$ , as  $\delta\xi \rightarrow 0$ . Since  $\mathbf{n}$  is independent of  $\lambda$  (except at  $\lambda = 0$ ), each sheet of the surface (50) is developable, and can be generated by folding a piece of paper. In applications, one considers portions of the surface (50) with  $\lambda < 0$  or  $\lambda > 0$ , to avoid inclusion of the singular locus defined by  $\lambda = 0$ .

## 4.2 Principal normal surface

The principal normal surface has rulings along the principal normal vectors to the curve  $\mathbf{r}(\xi)$ , and thus has the parameterization

$$\mathbf{s}(\xi, \lambda) = \mathbf{r}(\xi) + \lambda \mathbf{p}(\xi). \quad (51)$$

Since  $\mathbf{s}_\xi = \sigma[(1 - \lambda\kappa)\mathbf{t} + \lambda\tau\mathbf{b}]$  and  $\mathbf{s}_\lambda = \mathbf{p}$ , the surface normal is as

$$\mathbf{n} = \frac{\mathbf{s}_\xi \times \mathbf{s}_\lambda}{|\mathbf{s}_\xi \times \mathbf{s}_\lambda|} = \frac{(1 - \lambda\kappa)\mathbf{b} - \lambda\tau\mathbf{t}}{\sqrt{(1 - \lambda\kappa)^2 + (\lambda\tau)^2}} = \frac{\mathbf{b} - \lambda\boldsymbol{\omega}}{|\mathbf{b} - \lambda\boldsymbol{\omega}|},$$

where  $\boldsymbol{\omega}$  is the Darboux vector defined by (5). Note that  $\mathbf{n}$  is non-singular at  $\lambda = 0$ . Since  $\mathbf{n}$  depends explicitly on  $\lambda$ , the surface (51) is not developable.

If the curve has vanishing torsion at  $\xi = \xi_*$ , the surface normal becomes singular at the point  $\lambda = 1/\kappa(\xi_*)$  of the corresponding ruling — this identifies



the *center of curvature* for the curve point  $\mathbf{r}(\xi_*)$ . If the curvature is finite, the surface normal  $\mathbf{n}$  is non-singular at each point of the curve  $\mathbf{r}(\xi)$ .

On non-developable ruled surfaces, neighboring generators at parameter values  $\xi$  and  $\xi + \delta\xi$  do not intersect as  $\delta\xi \rightarrow 0$ , so there is no edge of regression. Instead, closest points on neighboring generators as  $\delta\xi \rightarrow 0$  define a locus called the *line of striction*. For the surface (47), it is defined [30, 32] by

$$\mathbf{q}(\xi) = \mathbf{r}(\xi) - \frac{\mathbf{r}'(\xi) \cdot \mathbf{d}'(\xi)}{|\mathbf{d}'(\xi)|^2} \mathbf{d}(\xi). \quad (52)$$

For the tangent surface, choosing the tangent  $\mathbf{t}(\xi)$  for  $\mathbf{d}(\xi)$  gives  $\mathbf{q}(\xi) = \mathbf{r}(\xi)$  — i.e., the line of striction is the edge of regression. However, for the principal normal surface, choosing  $\mathbf{p}(\xi)$  for  $\mathbf{d}(\xi)$  gives the line of striction

$$\mathbf{q}(\xi) = \mathbf{r}(\xi) + \frac{\kappa(\xi)}{\kappa^2(\xi) + \tau^2(\xi)} \mathbf{p}(\xi).$$

The *pitch* of a non-developable ruled surface is a measure of the variation of the surface tangent plane along each ruling. If  $\delta\theta$  and  $\delta h$  are the angle and distance between rulings at  $\xi$  and  $\xi + \delta\xi$ , the pitch  $p(\xi)$  is [22] the limit of the ratio  $\delta\theta/\delta h$ , as  $\delta\xi \rightarrow 0$ . For the surface (47), it is specified [30] by

$$p(\xi) = \frac{|\mathbf{d}'(\xi)|^2}{\mathbf{r}'(\xi) \cdot [\mathbf{d}(\xi) \times \mathbf{d}'(\xi)]}. \quad (53)$$

One can verify that, for the principal normal surface,  $p = (\kappa^2 + \tau^2)/\tau$ .

### 4.3 Rotation-minimizing ruled surface

For the tangent surface (50) and principal normal surface (51), the angular velocity  $\boldsymbol{\omega}$  of the rulings is defined by the Darboux vector (5), in which the term  $\kappa \mathbf{b}$  specifies an “unnecessary” rotation in the osculating plane — i.e., it is not required for the tangent plane of  $\mathbf{s}(\xi, \lambda)$  to be coincident with the osculating plane of  $\mathbf{r}(\xi)$  at each point. A *rotation-minimizing ruled surface*, interpolating a given curve and its osculating planes, can be defined by using one of the basis vectors (10)–(11) to specify the rulings, so as to eliminate the term  $\kappa \mathbf{b}$  in the Darboux vector. For example, the rulings of the surface

$$\mathbf{s}(\xi, \lambda) = \mathbf{r}(\xi) + \lambda \mathbf{f}(\xi), \quad (54)$$

have the angular velocity (12). The surface derivatives are  $\mathbf{s}_\xi = \sigma \mathbf{t} + \lambda \mathbf{f}'$  and  $\mathbf{s}_\lambda = \mathbf{f}$ , where  $\mathbf{f} = \cos \theta \mathbf{t} + \sin \theta \mathbf{p}$  and  $\mathbf{f}' = \sigma \tau \sin \theta \mathbf{b}$ . Hence, we have  $\mathbf{s}_\xi \times \mathbf{s}_\lambda = \sigma \sin \theta (\mathbf{b} + \lambda \tau \mathbf{f})$ , and the unit surface normal is defined by

$$\mathbf{n} = \frac{\mathbf{s}_\xi \times \mathbf{s}_\lambda}{|\mathbf{s}_\xi \times \mathbf{s}_\lambda|} = \text{sign}(\sin \theta) \frac{\mathbf{b} + \lambda \tau \mathbf{g}}{\sqrt{1 + \lambda^2 \tau^2}}. \quad (55)$$

Because the surface normal varies with  $\lambda$ , the surface (54) is not developable.

The surface normal (55) is singular along each ruling at a parameter value  $\xi$  for which the angle (11) is an integer multiple of  $\pi$  — i.e., at points where the ruling direction  $\mathbf{f}$  is parallel or anti-parallel to the tangent. Since the curvature is non-negative, the angle (11) is monotone-increasing with  $\xi$ , and such singular rulings occur at points on  $\mathbf{r}(\xi)$  determined by its curvature. In practice, one would restrict the surface (54) to intervals between such points: the integration constant  $\theta_0$  in (11) can be used to adjust such intervals.

**Proposition 6.** *The line of striction on the ruled surface (54) coincides with the curve  $\mathbf{r}(\xi)$ , as for the tangent surface. The pitch of this surface is equal to the torsion of the curve  $\mathbf{r}(\xi)$ , and is the smallest possible for the ruled surfaces defined by (47)–(48), whose tangent planes coincide with the osculating plane of  $\mathbf{r}(\xi)$ . These results also hold if the frame vector  $\mathbf{f}$  is replaced by  $\mathbf{g}$  in (54).*

**Proof :** Choosing  $\mathbf{d}(\xi) = \mathbf{f}(\xi)$  in (52), and recalling that  $\mathbf{f}' = \sigma \tau \sin \theta \mathbf{b}$ , we obtain  $\mathbf{r}' \cdot \mathbf{f}' = \sigma^2 \tau \sin \theta \mathbf{t} \cdot \mathbf{b} = 0$ , and hence  $\mathbf{q}(\xi) = \mathbf{r}(\xi)$ . Similarly, with  $\mathbf{d}(\xi) = \mathbf{f}(\xi)$  in (53), we have  $|\mathbf{f}'|^2 = \sigma^2 \tau^2 \sin^2 \theta$ , and

$$\mathbf{r}' \cdot (\mathbf{f} \times \mathbf{f}') = \sigma \mathbf{t} \cdot [(\cos \theta \mathbf{t} + \sin \theta \mathbf{p}) \times \sigma \tau \sin \theta \mathbf{b}] = \sigma^2 \tau \sin^2 \theta,$$

and hence  $p = \tau$ . Moreover, substituting (48) into (53) and simplifying gives

$$p = \tau + \frac{(\Theta' + \sigma \kappa)^2}{\sigma^2 \tau \sin^2 \Theta}.$$

This expression is of least magnitude when  $\Theta' = -\sigma \kappa$ , i.e.,  $\Theta(\xi)$  coincides with the angle  $\theta(\xi)$  specified by (11), identifying the RMOF vector  $\mathbf{f}(\xi)$ . ■

**Example 2.** Figure 3 illustrates the three types of ruled surfaces discussed above, in the case where the curve  $\mathbf{r}(\xi)$  is a segment of the circular helix (13). For all three ruled surfaces, the tangent plane coincides with the osculating plane along the helix, but the rotation-minimizing ruled surface exhibits the least possible angular velocity of its rulings consistent with this constraint.

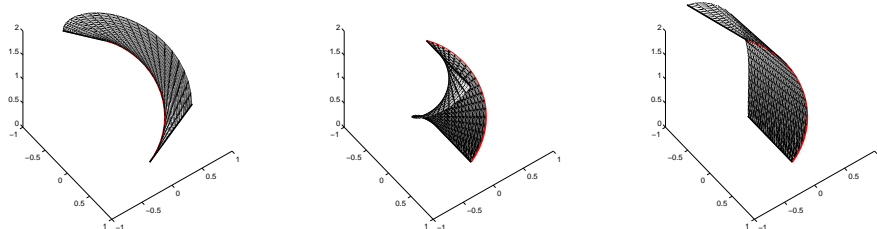


Figure 3: Comparison of tangent developable (left), principal normal surface (center) and rotation–minimizing ruled surface (right) for the circular helix (13) with  $R = \frac{1}{2}$  and  $k = \frac{1}{2}$  on the parameter domain  $\phi \in [0, \pi]$ .

**Remark 5.** The pitch provides a convenient way of piecing together portions of two non–developable ruled surfaces, with  $G^1$  continuity [22]. A generator is chosen from each surface, having equal pitch values. Then, if these generators are placed in coincidence, such that the points of striction are coincident, and the surface tangent planes are in agreement at this point, the two surfaces will possess a common tangent plane along the common generator. The rotation–minimizing ruled surfaces (54) are particularly amenable to this construction, because of the simple nature of their pitch and lines of striction.

**Example 3.** Consider the composite curve that consists of (i) the PH cubic  $\mathbf{r}(\xi)$  in Section 3.3 with  $\mathbf{p}_0 = (0, 0, 0)$ ,  $L_0 = L_2 = 2$ ,  $\vartheta = \frac{1}{2}\pi$ , and  $\varphi = \frac{3}{2}\pi$  for  $\xi \in [0, \frac{1}{2}]$ ; and (ii) the circular helix  $\mathbf{s}(\phi) = \Delta\mathbf{p} + f(-\cos\phi, -\sin\phi, \phi)$  with  $\Delta\mathbf{p} = (17, 1, \sqrt{2}(4 - \frac{3}{4}\pi))/8$  and  $f = 3\sqrt{2}/8$  for  $\phi \in [\frac{1}{4}\pi, \frac{3}{4}\pi]$ . These curves have a common end–point  $\mathbf{r}(\frac{1}{2}) = \mathbf{s}(\frac{1}{4}\pi) = \frac{1}{4}(7, -1, 2\sqrt{2})$  and a coincident tangent  $\mathbf{t} = \frac{1}{2}(1, -1, \sqrt{2})$ , curvature  $\kappa = 2\sqrt{2}/3$ , and torsion  $\tau = 2\sqrt{2}/3$  at this point, but the principal normal and binormal of  $\mathbf{s}(\phi)$  have opposite sense to those of  $\mathbf{r}(\xi)$ . For this composite curve, Figure 4 compares the principal normal surface, which is only  $G^0$  along the common ruling, and the rotation–minimizing ruled surface, which is  $G^1$  along the common ruling.

## 5 Closure

The variation of the Frenet frame, comprising the tangent  $\mathbf{t}$ , principal normal  $\mathbf{p}$ , and binormal  $\mathbf{b}$ , characterizes the local geometry of a space curve. The

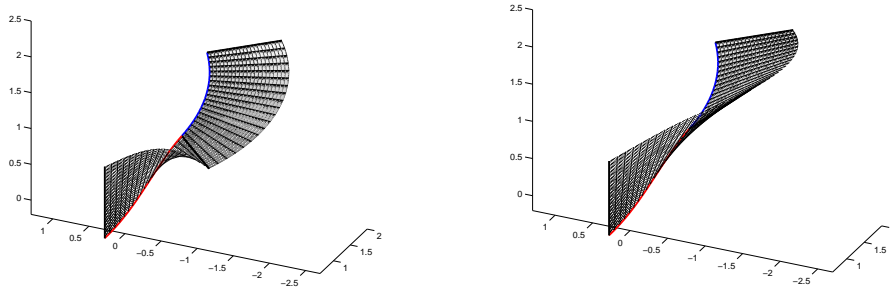


Figure 4: The principal normal surface (left) and rotation–minimizing ruled surface (right) for a composite curve, consisting of segments of a PH cubic (red curve) and a circular helix (blue curve). The rotation–minimizing ruled surface is tangent–plane continuous, but the principal normal surface is not.

Frenet frame is rotation–minimizing with respect to  $\mathbf{p}$  — i.e.,  $\mathbf{t}$  and  $\mathbf{b}$  have no rotation about  $\mathbf{p}$ . Rotation–minimizing *adapted* frames, characterized by normal–plane vectors  $\mathbf{u}$  and  $\mathbf{v}$  with no rotation about  $\mathbf{t}$ , are also well–known. The focus of this study has been on rotation–minimizing *osculating* frames, incorporating osculating–plane vectors  $\mathbf{f}$  and  $\mathbf{g}$  that have no rotation about the binormal  $\mathbf{b}$ . The vectors  $\mathbf{f}$ ,  $\mathbf{g}$  can be defined by rotating  $\mathbf{t}$ ,  $\mathbf{p}$  through an angle equal to minus the integral of the curvature with respect to arc length.

A comprehensive study of the existence of *rational* RMOFs on low–degree polynomial space curves indicates no cubic or quintic double PH curves with this property. The existence of rational RMOFs on degree 7 or higher–order curves remains an open problem. The use of RMOFs for the construction of a novel type of ruled surface, interpolating a space curve with tangent planes that are coincident with the osculating planes along the curve, and minimal rotation of the rulings under this constraint, was also investigated.

## Acknowledgement

The first author gratefully acknowledges financial support from the Gruppo Nazionale per il Calcolo Scientifico (GNCS) of the Istituto Nazionale di Alta Matematica Francesco Severi (INdAM).

## References

- [1] M. Barton, B. Jüttler, and W. Wang (2010), Construction of rational curves with rational rotation–minimizing frames via Möbius transformations, in *Mathematical Methods for Curves and Surfaces 2008*, LNCS 5862, pp. 15–25, Springer, Berlin.
- [2] E. Bayram, F. Güler, and E. Kasap (2012), Parametric representation of a surface pencil with a common asymptotic curve, *Comput. Aided Design* **44**, 637–643.
- [3] J. V. Beltran and J. Monterde (2007), A characterization of quintic helices, *J. Comput. Appl. Math.* **206**, 116–121.
- [4] L. Biard, R. T. Farouki, and N. Szafran (2010), Construction of rational surface patches bounded by lines of curvature, *Comput. Aided Geom. Design* **27**, 359–371.
- [5] R. L. Bishop (1975), There is more than one way to frame a curve, *Amer. Math. Monthly* **82**, 246–251.
- [6] H. I. Choi and C. Y. Han (2002), Euler–Rodrigues frames on spatial Pythagorean–hodograph curves, *Comput. Aided Geom. Design* **19**, 603–620.
- [7] H. I. Choi, D. S. Lee, and H. P. Moon (2002), Clifford algebra, spin representation, and rational parameterization of curves and surfaces, *Adv. Comp. Math.* **17**, 5–48.
- [8] M. V. Cook (1997), *Flight Dynamics Principles*, Arnold, London.
- [9] R. T. Farouki (2008), *Pythagorean–Hodograph Curves: Algebra and Geometry Inseparable*, Springer, Berlin.
- [10] R. T. Farouki (2010), Quaternion and Hopf map characterizations for the existence of rational rotation–minimizing frames on quintic space curves, *Adv. Comp. Math.* **33**, 331–348.
- [11] R. T. Farouki, C. Giannelli, C. Manni, and A. Sestini (2009), Quintic space curves with rational rotation–minimizing frames, *Comput. Aided Geom. Design* **26**, 580–592.

- [12] R. T. Farouki, C. Giannelli, C. Manni, and A. Sestini (2012), Design of rational rotation–minimizing rigid body motions by Hermite interpolation, *Math. Comp.* **81**, 879–903.
- [13] R. T. Farouki, C. Giannelli, and A. Sestini (2009), Helical polynomial curves and double Pythagorean hodographs I. Quaternion and Hopf map representations & II. Enumeration of low–degree curves, *J. Symb. Comput.* **44**, 161–179 & 307–332.
- [14] R. T. Farouki and C. Y. Han (2003), Rational approximation schemes for rotation–minimizing frames on Pythagorean–hodograph curves, *Comput. Aided Geom. Design* **20**, 435–454.
- [15] R. T. Farouki, C. Y. Han, C. Manni, and A. Sestini (2004), Characterization and construction of helical polynomial space curves, *J. Comput. Appl. Math.* **162**, 365–392.
- [16] R. T. Farouki and T. Sakkalis (1994), Pythagorean–hodograph space curves, *Adv. Comp. Math.* **2**, 41–66.
- [17] R. T. Farouki and T. Sakkalis (2010), Rational rotation–minimizing frames on polynomial space curves of arbitrary degree, *J. Symb. Comput.* **45**, 844–856.
- [18] R. T. Farouki and T. Sakkalis (2012), A complete classification of quintic space curves with rational rotation–minimizing frames, *J. Symb. Comput.* **47**, 214–226.
- [19] R. T. Farouki, N. Szafran, and L. Biard (2009), Construction of Bézier surface patches with Bézier curves as geodesic boundaries, *Comput. Aided Design* **41**, 772–781.
- [20] H. Guggenheimer (1989), Computing frames along a trajectory, *Comput. Aided Geom. Design* **6**, 77–78.
- [21] C. Y. Han (2008), Nonexistence of rational rotation–minimizing frames on cubic curves, *Comput. Aided Geom. Design* **25**, 298–304.
- [22] D. Hilbert and S. Cohn–Vossen (1952), *Geometry and the Imagination* (translated by P. Nemenyi), Chelsea (reprint), New York.

- [23] B. Jüttler and C. Mäurer (1999), Rational approximation of rotation minimizing frames using Pythagorean–hodograph cubics, *J. Geom. Graphics* **3**, 141–159.
- [24] F. Klok (1986), Two moving coordinate frames for sweeping along a 3D trajectory, *Comput. Aided Geom. Design* **3**, 217–229.
- [25] E. Kreyszig (1959), *Differential Geometry*, University of Toronto Press.
- [26] C–Y. Li, R–H. Wang, and C–G. Zhu (2011) Parametric representation of a surface pencil with a common line of curvature, *Comput. Aided Design* **43**, 1110–1117.
- [27] R. R. Martin (1983), Principal patches — A new class of surface patch based on differential geometry, *Eurographics '83* (P. ten Hagen, ed.), North–Holland, 47–55.
- [28] J. Monterde (2009), A characterization of helical polynomial curves of any degree, *Adv. Comp. Math.* **30**, 61–78.
- [29] M. Paluszny (2008), Cubic polynomial patches through geodesics, *Comput. Aided Design* **40**, 56–61.
- [30] H. Pottmann and J. Wallner (2001), *Computational Line Geometry*, Springer, Berlin.
- [31] J. Sánchez–Reyes and R. Dorado (2008), Constrained design of polynomial surfaces from geodesic curves, *Comput. Aided Design* **40**, 49–55.
- [32] D. J. Struik (1961), *Lectures on Classical Differential Geometry*, Dover Publications (reprint), New York.
- [33] W. Wang, B. Jüttler, D. Zheng, Y. Liu (2008), Computation of rotation minimizing frames, *ACM Trans. Graphics* **27**, No. 1, Article 2.